Poleward Force at the Kinetochore in Metaphase Depends on the Number of Kinetochore Microtubules

T. S. Hays and E. D. Salmon

Biology Department, University of North Carolina, Chapel Hill, North Carolina 27514

Abstract. To examine the dependence of poleward force at a kinetochore on the number of kinetochore microtubules (kMTs), we altered the normal balance in the number of microtubules at opposing homologous kinetochores in meiosis I grasshopper spermatocytes at metaphase with a focused laser microbeam. Observations were made with light and electron microscopy. Irradiations that partially damaged one homologous kinetochore caused the bivalent chromosome to shift to a new equilibrium position closer to the pole to which the unirradiated kinetochore was tethered; the greater the dose of irradiation, the farther the chromosome moved. The number of kMTs on the irradiated kinetochore decreased with severity of irradiation, while the number of kMTs on the unirradiated kinetochore remained constant and independent of chromosome-to-pole distance. Assuming a balance of forces on the chromosome at congression equilibrium, our results demonstrate that the net poleward force on a chromosome depends on the number of kMTs and the distance from the pole. In contrast, the velocity of chromosome movement showed little dependence on the number of kMTs. Possible mechanisms which explain the relationship between the poleward force at a kinetochore, the number of kinetochore microtubules, and the lengths of the kinetochore fibers at congression equilibrium include a "traction fiber model" in which poleward force producers are distributed along the length of the kinetochore fibers, or a "kinetochore motor–polar ejection model" in which force producers located at or near the kinetochore pull the chromosomes poleward along the kMTs and against an ejection force that is produced by the polar microtubule array and increases in strength toward the pole.

CHROMOSOMES are pulled toward the spindle poles by forces at their kinetochores generated in association with the kinetochore microtubules (kMTs).[1] kMTs also mechanically link chromosomes to the spindle poles in a bipolar orientation (2, 34). According to Ostergren (37), poleward force on a chromosome increases with distance from the pole. Paired chromosomes congress to the spindle equator because this is the position where opposing forces are balanced (18, 29). Evidence for this force-balance theory can be seen when the chromosomes are disconnected either naturally at anaphase (1) or artificially at metaphase (55); disjoined chromosomes are pulled towards opposite spindle poles as their kinetochore fibers shorten.

We previously tested Ostergren's hypothesis by analyzing the metaphase positions of multivalent chromosomes (more than two kinetochores) during first meiosis of grasshopper spermatocytes (10). At metaphase, multivalent chromosomes became positioned closer to the pole that had the larger number of connecting kinetochore fibers. We found that the sum of the lengths of kinetochore fibers to one pole was approximately equivalent to the sum of the lengths of the kinetochore fibers to the opposite pole. If the only forces on a chromosome occur at kinetochores, this result suggests that poleward force (F) at a single kinetochore is related to kinetochore-to-pole distance, or kinetochore fiber length (L), by the expression

$$F = kL \quad (1)$$

The constant k, a proportionality constant that is independent of length, appeared to be identical for all the kinetochores (10).

In the present study, we have explored further the validity of Eq. 1 and consider how the factor k, in particular, may be related to the number of kMTs for meiosis I chromosomes of grasshopper spermatocytes at metaphase. A 0.25-μm laser beam (23) was used to modify the normal balance in number of kMTs between opposing homologous kinetochores by selectively damaging one kinetochore complex. After irradiation, the bivalent congressed towards the pole faced by the unirradiated kinetochore. After a new equilibrium position was reached, the cell was fixed for electron microscopy. The number of kMTs for each kinetochore of an irradiated chromosome was determined from serial section electron micrographs and related to the length of the kinetochore fibers at congression equilibrium. Assuming a balance of forces at congression equilibrium, our results demonstrate that the net poleward force on a chromosome depends both on the number of kMTs as well as distance from the pole.

T. S. Hay's present address is Department of Genetics and Cell Biology, University of Minnesota, St. Paul, MN 55108.

1. *Abbreviation used in this paper*: kMT, kinetochore microtubule.

© The Rockefeller University Press, 0021-9525/90/02/391/14 $2.00

Materials and Methods

Preparation of Cell Cultures for Light Microscopy

A previously described method for light microscopy of living spermatocyte cultures was used with slight modification (35). Young adult males of *Melanoplus* were collected on or near the campus of the University of California at Irvine in September; *Dissosteria carolina* were collected in the vicinity of Chapel Hill, NC. For both species, testes were dissected in buffered saline as described by Nicklas and Staehly (34). The fat body adhering to the testis follicles was removed. Several follicles were separated from the testis and submerged in halocarbon oil (Halocarbon Products Corp., Hackensack, NJ) to prevent desiccation. Filter paper fragments were used to blot excess saline from the follicles while they were under oil. Subsequently, the follicles were transferred to a well slide containing fresh halocarbon oil, the follicles were cut, and the released spermatocytes were spread across the coverslip. The cells selected for experiments were judged to be normal and healthy using criteria of spindle size and shape, mitochondrial distribution, and, when possible, the successful completion of anaphase.

Microbeam Irradiation

The laser microbeam system used in this study is part of the National Institutes of Health's Laser Microbeam Program (LAMP) facility located at the University of California at Irvine and has been described in detail elsewhere (3). The 532-nm, second harmonic wavelength of a 10^6 W, pulsed neodynium-Yag (yttrium-aluminum-garner) laser was passed through attenuation filters into an inverted microscope (Axiomat; Carl Zeiss, Inc., Thornwood, NY), and focused to a spot size of $\sim$0.25 μm in diameter using 100× (1.3 NA) phase-contrast or differential interference contrast objectives (Carl Zeiss, Inc.). The duration of the laser pulse was 10 ns, and after attenuation the energy of the focused microbeam at the specimen plane ranged from 1.33 to 4.82 × 10^{-7} joules/pulse. Typically, kinetochores were irradiated with 2–6 pulses of the microbeam under control of an electronic shutter (Vincent Associates, Rochester, NY). The number of pulses of the laser and the exact positioning of the kinetochore relative to the focused microbeam were varied in order to control the extent of kinetochore damage.

The kinetochore region of each meiotic chromosome consists of two sister kinetochores (Fig. 1). The pair of adjacent sister kinetochores is $\sim$1 μm wide and can be resolved by phase-contrast or differential interference contrast optics. Focusing the laser microbeam onto a targeted kinetochore was facilitated by enhancing the microscope optical image using a television camera (model LST-1; Sierra Scientific, Mountain View, CA) and a real-time video image processing computer (DeAnza, Inc., San Jose, CA). A rolling average of 4–6 video frames was used to suppress the noise in the video image that is induced by effects from the pulsing laser.

Meiotic cells in mid to late prometaphase were viewed on the television monitor, and chromosomes in the focal plane closest to the coverslip were selected for irradiation. The kinetochore region of a chromosome to be irradiated was positioned at a computer-generated video crossbar that marked the position of the focused microbeam.

Photographic and Video Recording

The behavior of bivalents after the irradiation of kinetochores was viewed on the television monitor and recorded on a Sony TV09000 video time lapse recorder (Standard Theatre, Greensboro, NC) equipped with a Vicom time/data generator. In addition, 35-mm photographic records were made through the microscope at various times during an experiment.

Computer Analysis and Measurements

For 25 cells, chromosome behavior after kinetochore irradiation was analyzed using a video analyzer built according to the design of the video analyzer (model 321; Colorado Video Inc., Boulder, CO; see also reference 46). The voltage analogs for the x,y positional coordinates of kinetochores and spindle poles were digitized from individual video files into an Apple Computer using an 8-bit analog-to-digital converter (model AI-02; Interactive Structures, Bala Cynwyd, PA). Kinetochores were identified by the slight differences in phase density between a kinetochore and adjacent chromatin; spindle poles were identified by the phase-dense image of the centriole complex.

The digitized x,y position was analyzed by a computer algorithm to calculate the pole-to-pole and kinetochore-to-pole lengths. Lengths were plotted on a Laserwriter II (Apple Computer, Inc., Cupertino, CA) printer (see Fig. 2 *c*).

Video Analysis of Kinetochore Fiber Birefringence

The birefringent retardation of opposing kinetochore fibers of meiotic bivalents in *Dissosteria carolina* spermatocytes was observed using high-extinction, video-enhanced, polarization optics on an inverted optical bench microscope built according to a published design of Inoué (14). Video records were made and birefringent retardation intensities along corresponding lengths of homologous kinetochore fibers were measured using a video analyzer in a "line scan" mode to access the video voltages (14, 46). The voltages along a cursor line aligned with the long axis of a kinetochore fiber were digitized (digitizer model: A/D + D/A Board; Mountain Computer, Inc., Scotts Valley, CA) into an Apple II Plus computer; the magnitude of the background voltages in an adjacent region outside the spindle were subtracted. The voltages along the kinetochore fiber were normalized by the highest value.

Electron Microscopy

Irradiated bivalents were observed in living cells, then fixed at desired times and processed for electron microscopy by methods developed by Nicklas et al. (35, 36). In brief, this involved microinjection of fixative near the cell of interest and further processing and flat embedding in Epon. Our fixative contained agar-treated glutaraldehyde in a Pipes-buffered saline (36). 80–100-nm thick serial sections were cut in a plane longitudinal to the spindle axis. Sections were mounted and stained by standard procedures (17). Electron micrographs of serial sections were made on 70-mm roll film at a magnification of 3,100–3,200 using an electron microscope (model 10CA; Carl Zeiss, Inc.) operated at 80 kV.

Two-dimensional reconstructions of 11 chromosomes and the microtubules near their kinetochores were made using procedures that are described in detail elsewhere (36). The 11 chromosomes included 8 arbitrarily chosen from among 10 irradiated bivalents in one cell and 3, each from a different cell, 2 of which were controls. Serial sections were projected at 31× the original EM magnification onto the screen of the aerial viewer (Hoppman Corp., Springfield, VA), and the microtubules and chromosome outlines seen in the image were traced onto transparent polyester plastic sheets. The completed set of tracings was stacked in sequence; in stacking the tracings, profiles of microtubules that obviously continued through two or more sections were brought into the closest possible end-to-end alignment; i.e., the microtubules themselves served as registration aids (36). Non-kMTs were included only when necessary to facilitate registration of adjacent tracings, so only a fraction of the non-kMT populations is included in the reconstructions. For illustrations, a composite of the stacked tracings was made and photographed (see Figs. 5 *d*, 6, *a* and *b*, and 8 *a–c*). In these composites, all kMTs (*solid lines*) are shown, the few non-kMTs included are represented as dotted lines, and only some chromosome outlines are included.

Two observers, working independently on the tracings, counted the number of microtubules that inserted at the kinetochore region of the chromosomes. Two problems limited the accuracy of these counts. First, for some irradiated kinetochores, the normally distinct structure of the kinetochore was disrupted and more diffuse. Second, for unirradiated kinetochores the density of microtubules at the kinetochore made tracking and distinguishing individual microtubules difficult. Uncertainties in microtubule counts were recorded during the tracing procedure. The microtubule counts are, on average, reliable to within 11% for irradiated kinetochores and 6% for unirradiated kinetochores as estimated from the ratio of the maximum number of uncertain kMTs to those microtubules scored as kMTs by both observers (see Table I). Similar estimates of error for a comparable task have been reported by Nicklas and Gordon (33).

The stable equilibrium positions of irradiated bivalents and the respective kinetochore-to-pole distances (i.e., fiber lengths) were also determined from micrographs of a complete set of serial sections through the cell. Postirradiation positions of bivalents were assumed stable if they remained unchanged for 20 min or longer. A potential problem in the determination of these distances was their alteration during fixation and processing of cells for electron microscopy. Gross changes due to variation in the compression of sections would have been detected during reconstruction and were not observed. Otherwise, we have estimated a 10% error in these length measurements by comparing, for four of the analyzed bivalents, the kinetochore-to-pole distances determined from the electron micrographs with the same distances measured in light micrographs of the cell just before fixation.

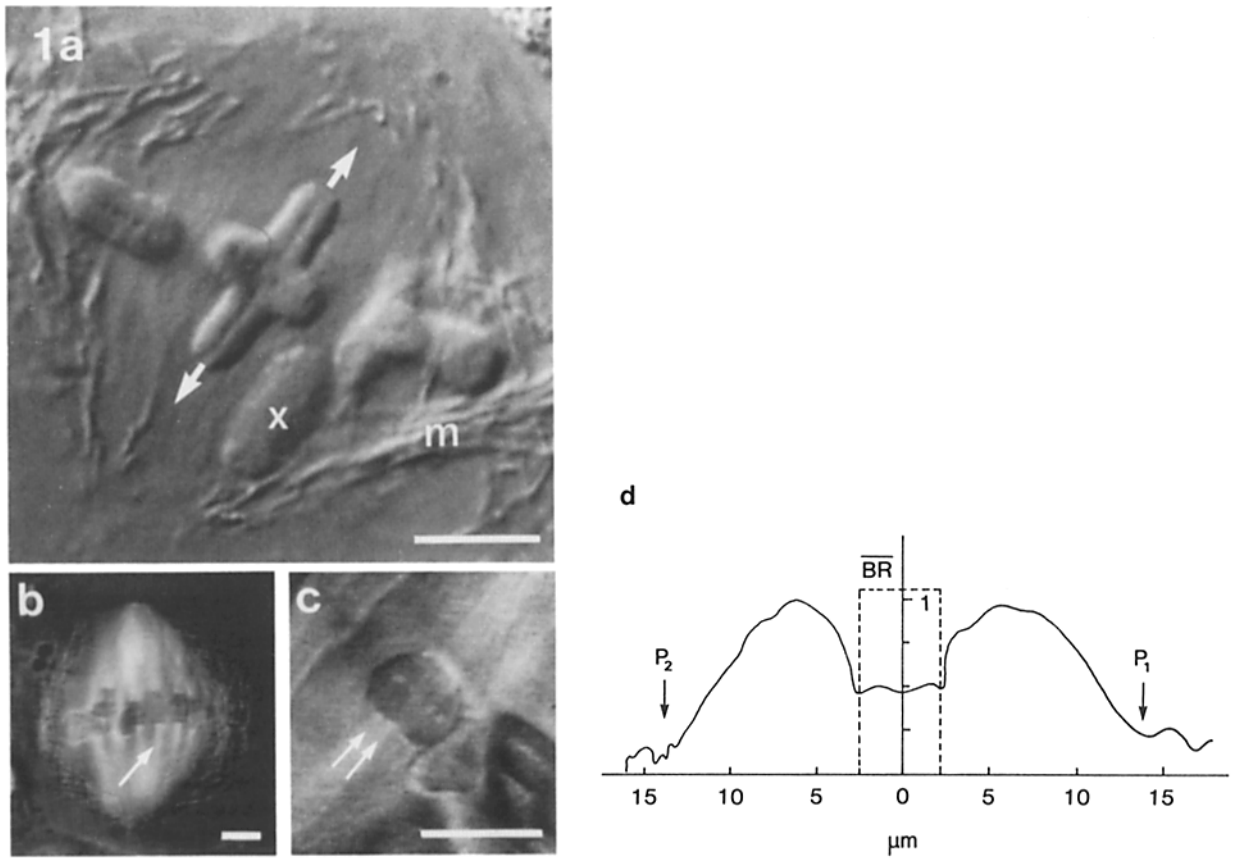

Figure 1. First meiotic division in grasshopper spermatocytes, metaphase spindles. (*a*) Meiotic bivalent chromosomes aligned at the spindle equator. The kinetochore regions (at base of arrows) of a typical cross-shaped bivalent are oriented towards opposite spindle poles. The sex univalent (*X*) lies in the lower half spindle. Mitochondria (*m*) outline the spindle. Differential interference microscopy. (*b* and *c*) Birefringent kinetochore fibers; polarization microscopy, photo of individual video frames. In *b*, kinetochore fibers (*arrow*) extend poleward from the kinetochores of fully congressed bivalents. In *c*, the two kinetochore fibers of one chromosome (*arrows*) are resolved using video contrast enhancement. (*d*) The profiles of birefringent retardation (*BR*) along the opposed kinetochore fibers of a single bivalent are nearly identical. The birefringent retardation intensities along a fiber were determined from the corresponding voltages measured from video recordings. The birefringent retardation values plotted were normalized by the peak value. The bivalent lies at the spindle equator (X-axis; 0 μm) in the region delimited by dotted lines; beyond the spindle poles, P_1 and P_2, BR is low. Bars, 5 μm.

Results

Kinetochore Microtubules in Control Chromosomes

As prometaphase progresses and the bivalent chromosomes congress to the spindle equator at metaphase, distinct birefringent kinetochore fibers arise which extend between a kinetochore and the polar region that the kinetochore faces (Fig. 1 *b*). In meiotic bivalents, sister kinetochores in each homologue are adjacent, oriented in the same direction (Fig. 1 *c*), and act as a unit kinetochore complex; fibers of paired homologous chromosomes, or bivalents, are oriented toward opposite poles. The birefringence intensity profiles of homologous kinetochore fibers at metaphase are mirror images (Fig. 1 *d*; see also references 45, 48), which indicates that the number of microtubules in homologous kinetochore fibers is equivalent because birefringent retardation is proportional to the number of microtubules (13, 47). Previous ultrastructural observations of grasshopper bivalents have shown nearly equal numbers of microtubules inserted at the two homologous kinetochore complexes (e.g., 33, 36), and we have confirmed this observation in the present electron microscopy study. On average, 37 microtubules insert at each kinetochore complex in the grasshoppers used for this study (range, 31–43; sample, 16 kinetochore complexes in 4 cells). For two control bivalents, the percent difference in microtubule number between homologous kinetochores was <8% (Table I, control chromosomes). These results provided a baseline for analyzing the reduction in the number of kMTs after microbeam irradiation.

Change in Chromosome Position after Microbeam Irradiation

Bivalent chromosomes responded to irradiations (0.4–1.6 mjoules) of a kinetochore region with movement of the bivalent toward the pole to which the unirradiated kinetochore was attached (Fig. 2). The irradiated bivalents eventually achieved stable equilibrium positions before anaphase which were shifted from the spindle equator (Fig. 2, 74 min). How far a bivalent shifted after the microbeaming of a kinetochore region appeared to depend on the dosage of irradiation. In the example shown in Fig. 2, kinetochore A_2 received six microbeam pulses while kinetochore B_1 received four

Table I. Comparison of Kinetochore Fiber Lengths and Kinetochore Microtubule Number for Control and Irradiated Chromosomes at Metaphase

Cell	Chromosome ID	Spindle length	Kinetochore fiber length		Microtubules*		Difference in microtubule number ($[N_1 - N_2/N_1]100$)
			L_1	L_2	N_1	N_2	
		μm	μm	μm	n	n	%
Controls							
1	A	28	13.0	13.0	40(1)	43(1)	7
2	A	28	12.8	12.8	33(3)	32(1)	3
Irradiated							
2	B	28	7.2	15.5	42(2)	29(2)	13
	C	28	8.1	15.9	43	28(6)	34
	D	28	7.3	17.2	36(2)	21(2)	42
	E	28	5.0	17.5	40(3)	7(1)	90
	F	28	4.6	18.4	38(4)	12/6‡	84
	G	28	5.0	21.6	31(2)	5	93
	H	28	4.2	21.3	34	8/4‡	88
3	A	29	7.4	17.6	38(4)	19(8)	50
4	A	28	10.0	15.0	37(3)	25(2)	33

Kinetochores attached to the spindle pole, P_2, were irradiated.
* Maximal number of microtubules for which insertion at the kinetochore was uncertain; they were not counted as kMTs.
‡ Amphitelic orientation of irradiated kinetochores. Microtubules extended towards both poles. For analysis, we took the difference in microtubule number towards opposite poles, e.g., 12/6: 12 − 6 microtubules = 6 kMTs.

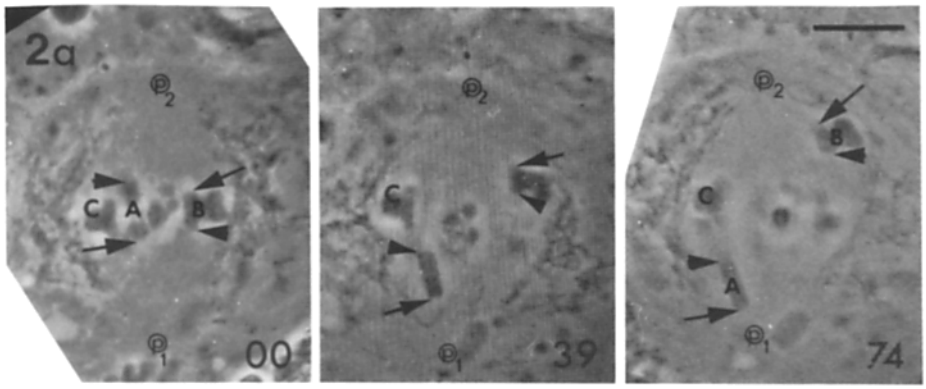

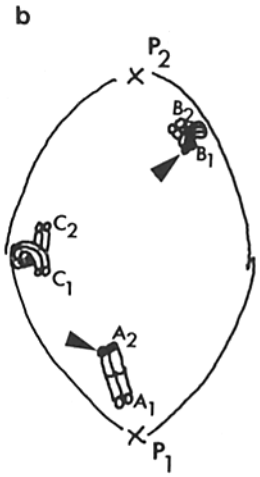

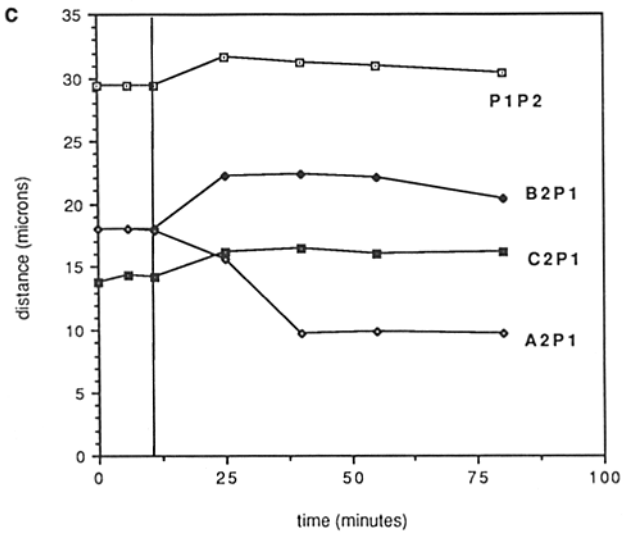

Figure 2. Chromosome behavior after kinetochore irradiation. (*a*) In this metaphase cell, two bivalents, A and B, were each irradiated at one kinetochore. Arrowheads mark the irradiated kinetochores, and arrows mark the unirradiated homologous kinetochores. Each frame is a photograph of one video frame; numbers indicate time after irradiation in minutes. As shown in the 39- and 74-min frames, both irradiated bivalents move toward the spindle pole to which the unirradiated kinetochore (*arrows*) is oriented. Unirradiated bivalents (e.g., bivalent C), remain at the spindle equator. Bar, 10 μm. (*b*) Schematic drawing of the cell in 74-min print showing the metaphase positions of the irradiated bivalents A and B, and control, unirradiated chromosome C. For each kinetochore, subscripts 1 and 2 indicate the pole toward which the kinetochore is oriented (e.g., kinetochore A_1 is oriented to pole P_1). Arrowheads mark the irradiated kinetochores. (*c*) Chromosome movements relative to pole P_1 after microbeam irradiation (*vertical bar*). The distances between the kinetochores A_2, B_2, and C_2, and the lower pole P_1 are plotted relative to time. Bivalent A, irradiated at kinetochore A_2, moved towards pole P_1 (distance A_2P_1 shortened), and then maintained a stable position ~10 μm from the pole. Bivalent B, irradiated at kinetochore B_1, moved away from P_1, and the distance B_2P_1 increased. The control bivalent C did not change position; C_2P_1 remained constant. The rates of movement were determined over the 15 min immediately after irradiation and were 0.21 and 0.20 μm/min for bivalents A and B, respectively. The distance between the two spindle poles is also plotted (P_1P_2).

pulses; bivalent A moved closer to pole P_1 than bivalent B moved toward P_2 (Fig. 2, *a–c*). When a single kinetochore region was irradiated with sufficient dosage (e.g., bivalent C in Fig. 3 *b*), that bivalent moved all the way to the opposite pole. We often observed a lateral displacement of bivalents as they traveled towards a pole, but this behavior was also observed in movements of unirradiated bivalents, so it is not a direct result of irradiation. Kinetochores that were only partially damaged by the microbeam functioned sufficiently well to segregate chromosomes during anaphase. An example is shown in Fig. 3 *a*. The irradiated bivalent was shifted off the metaphase plate; at anaphase the partner chromosomes separated, and both the partially damaged and the intact kinetochores moved toward their respective poles (Fig. 3 *a*: 0-, 22-, 87-, 113-min prints). In contrast, after extensive irradiation of an entire kinetochore, the kinetochore and its associated chromosome failed to segregate at anaphase (e.g., bivalent C in Fig. 3 *b*: 0-, 11-, 41-, 91-min prints), presumably because kinetochore complexes that have been completely damaged are devoid of kMTs.

For controls, we observed the effects of irradiations of the chromosome proper (but not the kinetochore), the kinetochore fiber (but not the kinetochore proper), and the cytoplasm. None of these irradiations elicited the behavior that typically followed irradiations of kinetochores.

In four experiments we attempted to irradiate a kinetochore fiber by positioning the focused microbeam 1–2 μm poleward from a kinetochore, along the presumed path of the kinetochore microtubules towards the pole. Fig. 4 *a* represents the most striking example. As shown, the bivalent whose kinetochore fiber was irradiated moved first toward the upper pole (P_1), away from the site of irradiation. Then, the bivalent moved towards the lower pole (P_2), towards the irradiated spot, and finally returned to the metaphase plate. In three other cases, the slight movements we observed after irradiation were difficult to distinguish from the normal oscillation of bivalents during congression.

The effect of targeting the microbeam on nonkinetochore regions of a chromosome is illustrated in Fig. 4 *b*. When we irradiated the chromatin midway between the opposed kinetochore regions of a bivalent, the chromosomes were stretched towards both poles. This result shows that both kinetochores are subject to poleward-directed forces. The increased elasticity of chromatin that results from irradiation allowed those forces to be expressed in the poleward movement of both kinetochores.

In all cases, the effect of irradiation was limited to the bivalent that was targeted. Unirradiated bivalents in the process of congressing or bivalents previously positioned at the metaphase plate were not affected by the irradiation of neighboring chromosomes. Irradiations outside the spindle region had no effect on bivalent behavior. Cell lysis was observed in some cases, but only after numerous microbeam pulses.

The rates of chromosome movement were not altered greatly by partial kinetochore irradiation. After irradiation, bivalent chromosomes moved to new equilibrium positions at an average rate of 0.2 μm/min (14 irradiated chromosomes, SD = 0.2, 0.06–0.40 μm/min, 20–22°C). This rate is of the same magnitude as observed for unirradiated bivalents during late prometaphase, the stage during which the experiments were performed. Chromosomes with partially irradiated kinetochores also moved poleward during anaphase at a velocity characteristic of normal chromosome movement (an average of 0.22 μm/min), and equivalent to the velocity of the unirradiated partner chromosome or other unirradiated chromosomes in the same cell (7 irradiated chromosomes, 7 unirradiated partner chromosomes, and 16 control chromosomes, SD = 0.07, 0.1–0.4, 20–22°C).

Changes in Kinetochore Structure and Microtubule Number as a Result of Microbeam Irradiation

Typcial changes after microbeam irradiation are shown in Fig. 5. The upper kinetochore region (*arrowhead*) of bivalent A was irradiated on the one side with a low dosage (0.8 mjoules) of microbeam irradiation. The bivalent proceeded to move a short distance toward the pole P_1 while adjacent bivalents remained stationary (Fig. 5, *a* and *b*; compare chromosomes A and B). A low magnification survey micrograph from one section of the series shows the irradiated bivalent in its new equilibrium position (Fig. 5 *c*) closer to the pole P_1 than the unirradiated neighboring bivalent (B) with which it was aligned before irradiation. The microbeam damage is apparent as a region of chromatin of lower electron opacity as described previously (23). We reconstructed the overall organization of the kinetochore fiber microtubules for both the irradiated bivalent A and the neighboring unirradiated bivalent B (Fig. 5 *d*). There are fewer microtubules attached to the irradiated kinetochore than to the unirradiated kinetochore of its partner chromosome or in the kinetochores of the neighboring bivalent B. For irradiated kinetochores, the general morphology of the kinetochore and surrounding chromatin is disrupted (e.g., Fig. 6 *e*), and the microtubules approaching the irradiated kinetochore appear less parallel than those approaching unirradiated kinetochores. Frequently, oblique microtubules cross the kinetochore fiber as shown in Fig. 6, *d* and *e*. The irradiated kinetochore had 33% fewer microtubules than the unirradiated homologous kinetochore for the example shown in Figs. 5 and 6 (see Table I; cell 4).

The Relation between Chromosome Position and the Number of kMTs

The two effects of kinetochore microbeam irradiation are (*a*) a change in the position of the bivalent between the spindle poles, a change which necessitates a compensatory change in the lengths of the kinetochore fibers of the bivalent; and (*b*) a decrease in the number of kinetochore microtubules at the irradiated kinetochore, with no change in the number of microtubules at the homologous unirradiated kinetochore. The relationship between kinetochore microtubule number and fiber length, derived from serial sections (Fig. 7) and two-dimensional reconstructions (Fig. 8), is plotted in Fig. 9. For the irradiated kinetochores, a regression analysis indicates an inverse dependence of kinetochore fiber length on the number of microtubules remaining attached to the damaged kinetochore (Fig. 9 *a*). For unirradiated kinetochores of homologs, however, the attached fibers shortened while the normal complement of microtubules (Fig. 9 *b*) remained unchanged.

Discussion

The behavior of chromosomes after microbeam irradiation

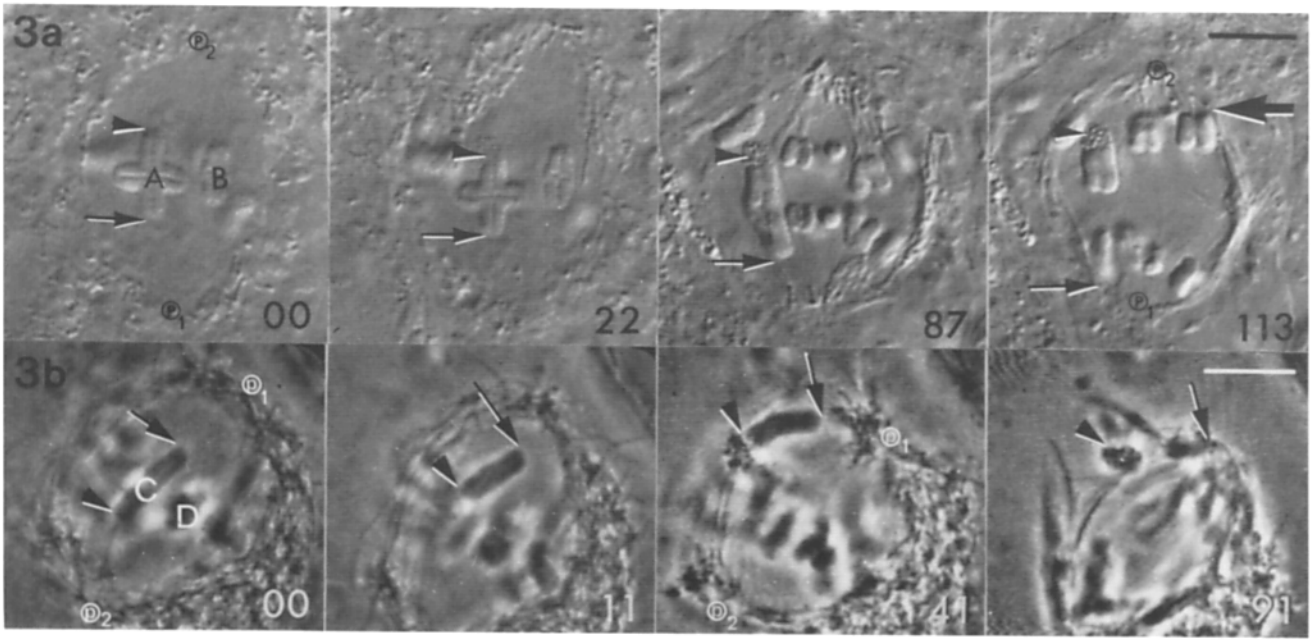
3a
A
B
00
22
87
113
3b
C
D
00
11
41
91

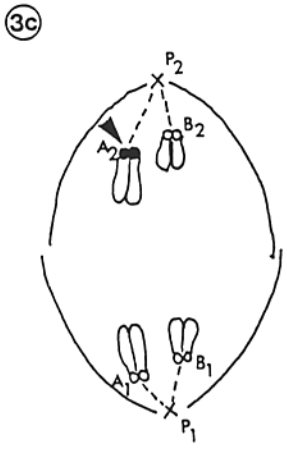
3c
P2
A2
B2
A1
B1
P1

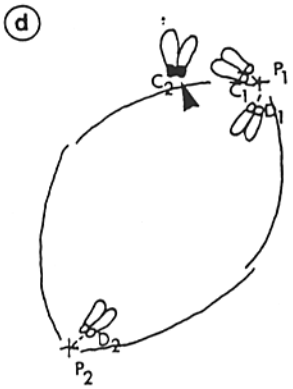
d
C2
C1
P1
P2

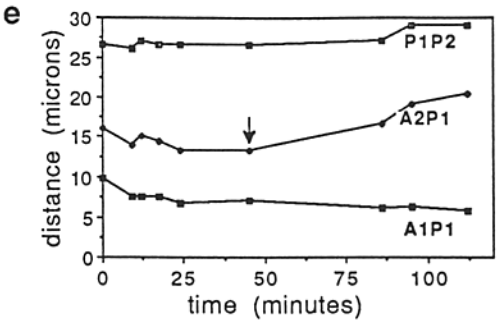
e
distance (microns)
time (minutes)
P1P2
A2P1
A1P1

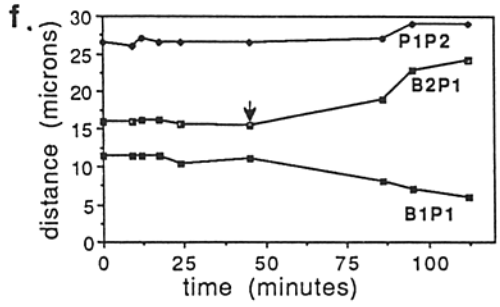
f
distance (microns)
time (minutes)
P1P2
B2P1
B1P1

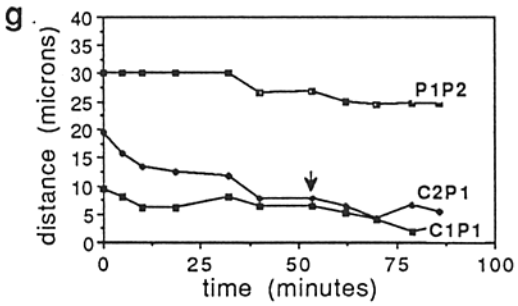
g
distance (microns)
time (minutes)
P1P2
C2P1
C1P1

has been studied by several other investigators (15, 23, 52). A consistent observation is that irradiation of one kinetochore causes the entire chromosome to move towards the pole to which the unirradiated kinetochore is attached. McNeill and Berns (23) found that irradiation of kinetochores on mitotic PtK_1 chromosomes could sever the connection to the pole, so that at metaphase the chromosome was pulled close to the pole to which the intact sister kinetochore was connected, or at anaphase the irradiated chromatid failed to move at all. We found similar results when a meiotic kinetochore complex was completely disrupted (Fig. 3 *b*). Because the grasshopper meiotic kinetochore complex is sufficiently large to permit partial disruption by the 0.25-μm-diam laser microbeam, we were able to show that a partially irradiated kinetochore remained functional (e.g., Fig. 3 *b*). A bivalent with one partially damaged kinetochore complex moved to a new equilibrium position that was closer to but not next to the pole to which the undamaged kinetochore complex was oriented (Fig. 2; reference 15). In such cases, the bivalents separated normally at anaphase and the disjoined chromosomes moved to the appropriate poles.

Such observations can be understood in terms of a force–balance mechanism of chromosome congression (10, 29, 37, 44) with antagonistic kinetochore poleward forces acting on the bivalent. At metaphase, the bivalent is under tension at the spindle equator. When a bivalent is irradiated between its opposed kinetochores, the stiffness of the interconnecting chromatin is reduced, but the integrity of the kinetochores is unaffected. Consequently, the chromosomes are stretched further towards both poles by the forces acting at the two kinetochores (Fig. 4 *b*). Irradiation of a kinetochore region reduces the magnitude of poleward force at that kinetochore compared to the opposing kinetochore complex. This force imbalance causes the bivalent to shift towards the pole to which the undamaged kinetochore is oriented until changes in the position of the bivalent between the spindle poles restore balance.

Our electron micrographs show that the distance a bivalent moves after kinetochore irradiation correlates with the reduction in microtubules. The fiber attached to the irradiated kinetochore elongates and the opposing fiber shortens. The fewer the number of microtubules remaining, the longer the associated kinetochore fiber becomes and the farther the chromosome moves towards the pole on the side of the undamaged kinetochore. This result suggests that each microtubule attached at a kinetochore represents a unit of poleward force. Thus, independent of the origins of poleward force production, the number of kMTs can be viewed as a measure of the functional strength of a kinetochore:

$$F = f(N), \tag{2}$$

where F is the magnitude of poleward force at a kinetochore and N is the number of kMTs.

Our observation that the complement of kMTs at the unirradiated kinetochore is independent of fiber length shows that the length of a kinetochore fiber is not simply a function of the number of kMTs at congression equilibrium. Rather, an imbalance of poleward forces on the bivalent induces changes in the position of the bivalent between the spindle poles and changes in the lengths of the kinetochore fibers until a new balance of poleward forces is established.

Both the velocity of bivalents during congression and the velocity of chromosomes during anaphase appear to be independent of poleward force at the kinetochore and the number of kMTs. However, chromosome movement is closely coupled with the lengthening and shortening of the kinetochore fibers. Nicklas (30, 31) has shown that the amount of force necessary to stall an anaphase chromosome in grasshopper spermatocytes is $\sim 7 \times 10^{-5}$ dyn, ~10,000 times greater than the drag force on the chromosome during normal anaphase chromosome movement (28). In our experiments, irradiated bivalents moved at velocities similar to normal bivalents in late prometaphase or separated chromosomes during anaphase (0.1–0.4 μm/min at 20–22°C). During anaphase a chromosome with a partially damaged kinetochore moved poleward at the same average velocity as the unirradiated partner chromosome. These data support arguments that chromosome velocity is independent of load and limited by the molecular mechanisms that govern the rate of kMT assembly or disassembly (42, 45).

Analysis of Congression Models

For any model to explain congression it must account for the interrelationship between the number of kMTs, the length of the kinetochore fiber, and the magnitude of poleward force

Figure 3. Partial vs. total kinetochore irradiation. (*a*) Part of the upper kinetochore (*arrowhead*) of bivalent A was irradiated (0 min); this resulted in a shift of the chromosome towards the pole P_1 (22 min). At anaphase, both kinetochores (*arrowhead* and *arrow*) and their associated chromosomes moved poleward (87 min) and segregated properly to opposite poles (113 min). Owing to the initial shift of the irradiated bivalent towards the lower pole, the irradiated chromosome lagged behind neighboring chromosomes during poleward anaphase movement. Unirradiated bivalents (e.g., B) divided normally. Differential interference contrast micrographs. Bar, 10 μm. (*b*) The entire face of the lower kinetochore (*arrowhead*) of bivalent C was irradiated (0 min). Subsequently (11 and 41 min), the bivalent moved to P_1, the pole to which the unirradiated kinetochore (*arrow*) was attached. At anaphase (91 min), the irradiated kinetochore (*arrowhead*) did not segregate properly to P_2, but remained near P_1. Phase-contrast micrographs. Bar, 10 μm. (*c* and *d*) Schematic drawings of the cells in *a* and *b*, respectively. The anaphase positions of the two partner chromosomes (e.g., A_1 and A_2) of irradiated bivalents A and C and unirradiated bivalents B and D are shown. Dashed lines indicate the kinetochore-to-pole distances. Arrowheads indicate the irradiated kinetochores. (*e*) Partial kinetochore irradiation, bivalent A. For 25 min after irradiation (0 min) the bivalent moved toward pole P_1, as indicated by a decrease in distances A_1P_1 and A_2P_1. It then maintained a stable position for ~25 min until anaphase (onset at arrow), when each partner chromosome (A_1 and A_2) moved towards its proper pole, with distance A_1P_1 decreasing and the distance A_2P_1 increasing. (*f*) No kinetochore irradiation, bivalent B. The kinetochore-to-pole distances remained fairly constant until anaphase (onset at *arrow*), when similar to bivalent A (see *c*), both chromosomes B_1 and B_2 segregated to opposite poles. (*g*) Total kinetochore irradiation, bivalent C. After irradiation at time D, both chromosomes C_1 and C_2 moved to pole P_1 as indicated by decreasing distances C_1P_1 and C_2P_1. During anaphase (onset at arrow), both chromosomes remained near P_1; chromosome C_2 did not segregate appropriately to P_2.

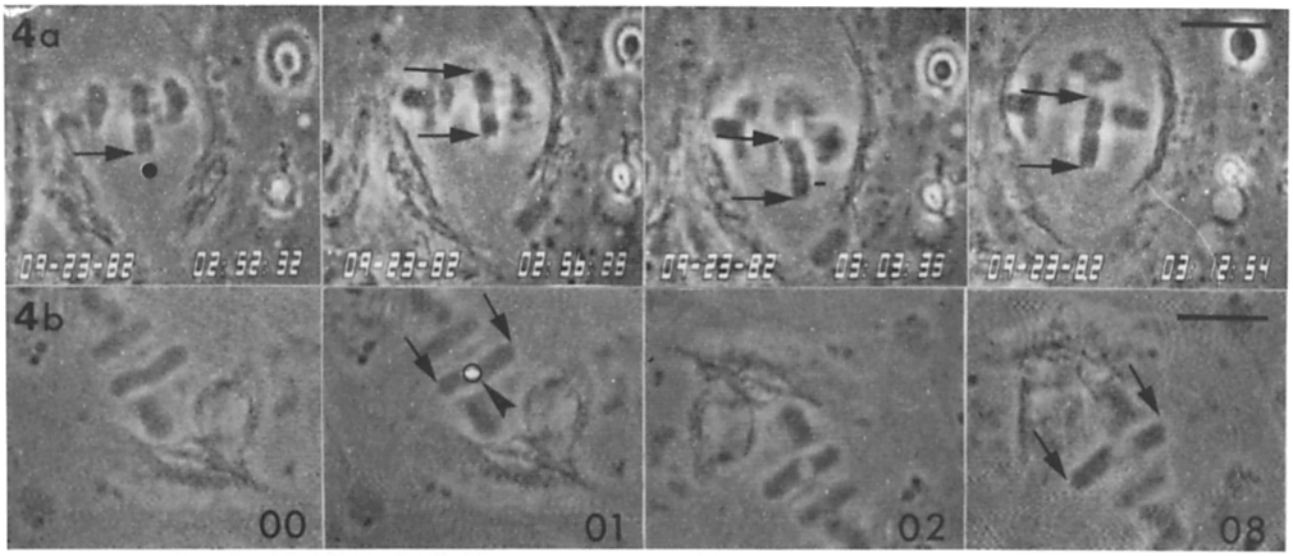

Figure 4. Control irradiations of a kinetocore fiber (*a*) or nonkinetochore region of the chromosome (*b*). (*a*) To irradiate a kinetochore fiber, the microbeam was aimed at an area (*solid dot*) 2 μm below the lower kinetochore and towards the lower pole (2:52:32). In response, the bivalent moved slightly towards the upper pole (2:56:28), then towards the lower pole (3:03:38), and finally moved back to the spindle equator (3:12:54). Photographs of video frames. Bars, 10 μm. (*b*) A region of chromatin (*white dot* and *arrowhead*) between the opposed kinetochores (*arrows*) was irradiated (1 min) and stretched (8 min) as the kinetochores were pulled towards opposite poles. Phase-contrast micrographs. Bars, 10 μm.

on a kinetochore. Possible mechanisms include force producers distributed along the lengths of kMTs, elastic contractile elements associated with kMTs, and force producers located at the kinetochores which pull the chromosome poleward against a counterforce emanating from the poles.

Although the lengths of microtubules which comprise the kinetochore fibers have not been determined, many kMTs probably extend continuously from kinetochore to pole (11, 39, 51, 56). Therefore, kinetochore-to-pole distance defines the maximum possible length of kMTs, and multiplication of the number of kMTs (N) by the length of the kinetochore fiber (L) gives an estimate of the total microtubule polymer associated with a kinetochore. To generate a poleward force proportional to LN, or to the total contour length of the microtubules attached to a kinetochore, molecular force producers which actively drive kMTs poleward could be uniformly distributed along the kMTs. Models proposing such mechanical cross-bridges between microtubules and microfilaments or between microtubules and the cytoplasmic matrix exemplify "traction fiber" models (21). In this regard the recent localization of kinesin in sea urchin mitotic spindles is provocative (49). Kinesin has been characterized as an ATPase that can bind to and actively push purified microtubules in the direction of their minus ends, which in spindles are proximal to the poles (49, 53).

In the above traction fiber model, the poleward force at a kinetochore is proportional to the number of kMTs (N) and the length of the kinetochore fiber (L):

$$F = cNL, \tag{3}$$

where c is a proportionality constant. If the only forces on the chromosome occur at kinetochores, the resultant force (RF) on a bivalent chromosome at congression equilibrium is given by

$$RF = c(N_1L_1 - N_2L_2) = 0, \tag{4}$$

where the subscripts denote the poles to which the kinetochores are oriented, and congression occurs by a force balance mechanism.

It follows, by algebraic manipulation of Eq. 4, that the ratio of kinetochore fiber lengths at congression equilibrium will equal the inverse ratio of the corresponding numbers of kMTs:

$$L_1/L_2 = N_2/N_1. \tag{5}$$

In Fig. 10, L_1/L_2 is plotted against N_2/N_1 for all 11 irradiated bivalents analyzed. Although the traction fiber model predicts a linear relationship, an exponential curve fits the data better than a straight line. The measurement error for L (10%) and N (11% for irradiated kinetochores, 6% for unirradiated kinetochores) may explain this discrepancy but, in any case, our results do not uniquely define the relation between force and kinetochore fiber length.

The tight coupling between chromosome movements and changes in kinetochore fiber lengths can be accommodated in traction fiber models. The kinetochore fibers are much stiffer than the chromosomes (27, 30). As a result, the majority of the force generated along the kinetochore fiber will be taken up by the stiffness of the fiber, and only a small fraction will be transmitted to the chromosome. The kMTs will normally be under a small amount of tension near the kinetochore and under compression over most of their length, where the magnitude of compression is greatest near the poles. This pattern of stress (tension or compression) along the fiber predicts that tubulin incorporation into kMTs occurs at the kinetochore and tubulin dissociation occurs near the pole (12, 31). At congression equilibrium, a steady flux of tubulin poleward through the kMTs would occur (19). Mitch-

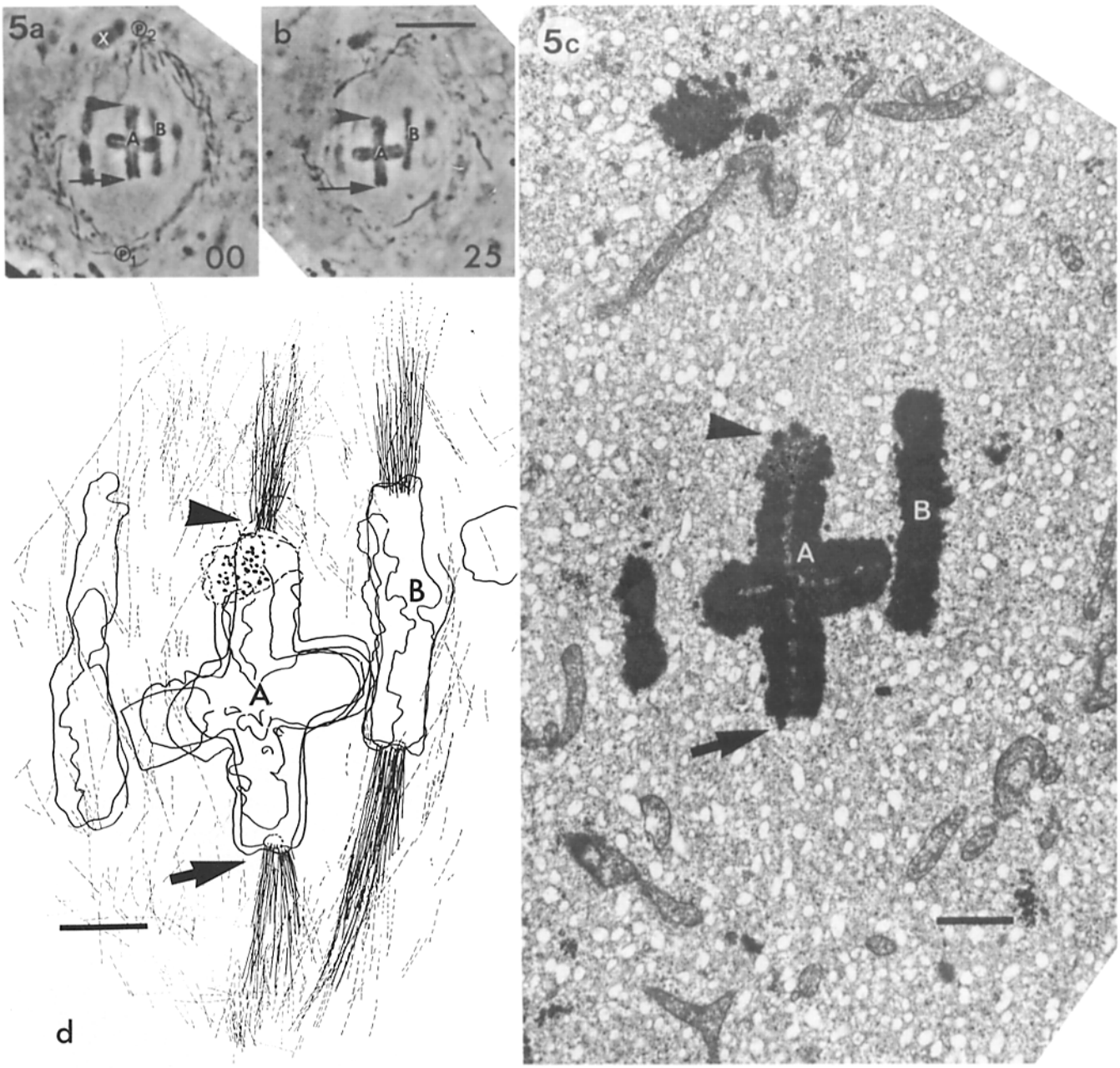

Figure 5. Light and electron microscopy of a cell subjected to kinetochore irradiation. (*a* and *b*) The living cell showing the positions of the irradiated (*arrowhead*) and unirradiated (*arrow*) kinetochores of one bivalent (*A*). In these phase-contrast micrographs, numbers indicate time in minutes after microbeam irradiation. (*a*) Immediately after irradiation (0 min), bivalent A lies at the spindle equator and is aligned with a neighboring unirradiated bivalent (*B*). (*b*) After 25 min the irradiated bivalent A had moved towards pole P_1, while the neighboring unirradiated bivalent (*B*) remained stationary. Bar, 10 μm. (*c*) The cell, fixed for electron microscopy at 35 min after irradiation. This survey electron micrograph shows the shifted irradiated bivalent A and the unirradiated bivalent B still at the spindle equator. Bar, 2 μm. (*d*) A two-dimensional reconstruction of the bivalents A and B, and their kinetochore microtubules. The irradiated kinetochore (*arrowhead*) has a thinner, narrower bundle of microtubules than the opposed homologous kinetochore or the kinetochores of the neighboring unirradiated bivalent B. Selected nonkinetochore microtubules are represented by the dotted lines. Bar, 2 μm.

ison (24, 25) and Mitchison and Kirschner (26) have presented evidence that tubulin incorporation occurs at the kinetochore in mitotic metaphase cells, and that a poleward flux of tubulin within kinetochore fibers occurs. However, the significance of this poleward tubulin flux is still controversial (8, 22, 24, 25).

When the number of kMTs is abruptly reduced at one kinetochore complex by irradiation, tension in the remaining microtubules will rise because fewer microtubules remain to support the pulling forces generated by the normal complement of microtubules in the opposing fiber. Concurrently, the microtubules near the kinetochore in the opposing fiber will bear a greater net compression than normal. This imbalance in stress along the microtubules may induce assem-

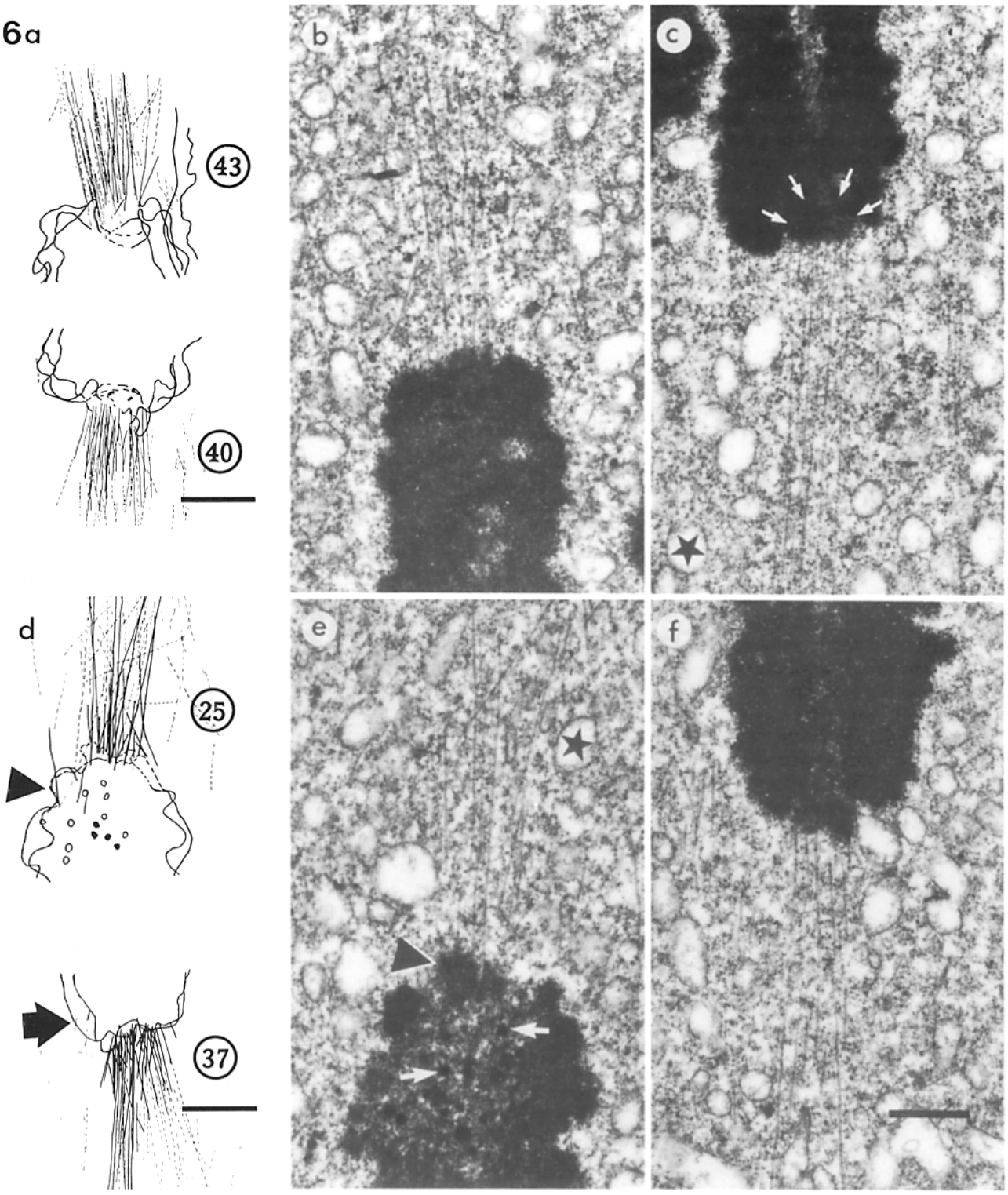

Figure 6. kMTs associated with normal (unirradiated) vs. irradiated kinetochores. (*a–c*) Unirradiated kinetochores of bivalent B of Fig. 5. (*a*) Reconstruction of the kinetochore regions from serial micrographs showing the number of microtubules inserting at each kinetochore (microtubule number in circles). (*b* and *c*) Representative electron micrographs of sections through the upper (*b*) and lower (*c*) kinetochore of bivalent B. The typical morphology of kinetochores is shown in *c* (*arrows*). (*d–f*) Kinetochores of irradiated bivalent A of Fig. 4. (*d*) Reconstruction of the irradiated (*arrowhead*) and unirradiated (*arrows*) kinetochores. The irradiated kinetochore (*arrowhead*) has a reduced complement of microtubules relative to the partner unirradiated kinetochore (*arrow*); see microtubule numbers in circles. (*e* and *f*) Representative electron micrographs through the upper (*e*) and lower (*f*) kinetochores of bivalent A. Chromatin surrounding the damaged kinetochore (*arrowhead*) is of lower electron opacity and is spotted with dense lesions (*white arrows*). Microtubules approaching the irradiated kinetochore (*e*) are less parallel in register compared with the unirradiated kinetochores (*b*, *c*, and *f*). Several microtubules run through the irradiated kinetochore fiber at oblique angles (*d*; *dotted lines*). Membrane vesicles are a prominent component within these spindles. Bars, 1 μm.

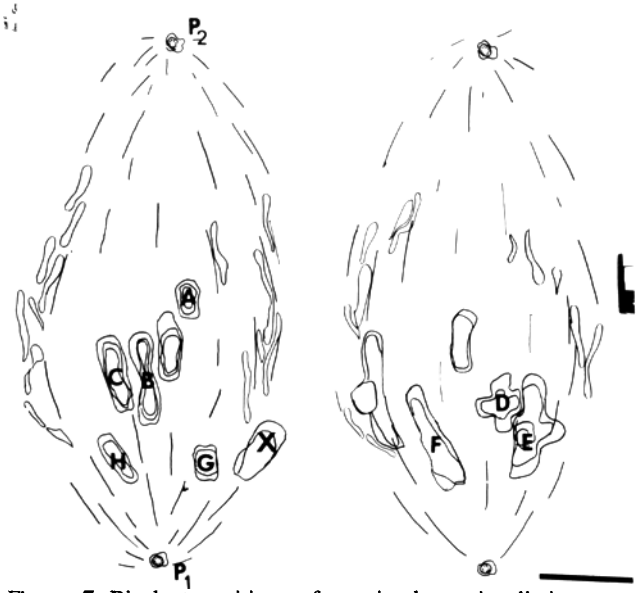

Figure 7. Bivalent positions after microbeam irradiation; two-dimensional reconstructions for two different levels in the spindle of cell 2. 10 of the 11 bivalents were irradiated at the kinetochore attached to the upper spindle pole (P_2); neither bivalent A nor the univalent sex chromosome (X) was irradiated. *A–H* indicate the bivalents for which kinetochore microtubule number and fiber lengths were determined (Table I, cell 2). Bar, 5 μm.

bly of the microtubules attached to the irradiated kinetochore and disassembly of the microtubules attached to the unirradiated kinetochore until new equilibrium lengths are achieved, when the poleward forces and stresses within the kinetochore fiber microtubules are balanced.

Although the traction fiber model explains much of the congression behavior of bivalent, multivalent, and irradiated chromosomes in bipolar spindles, alternative means of force production have been suggested, and there are experimental data which appear to be inconsistent with the traction fiber model. It has been suggested that actomyosin fibrils (6, 7), an elastic contractile entity that spans the kinetochore-to-pole distance (38, 50), or that dynein-like ATPases associated with the kinetochore corona (40; for review see reference 44) may apply motive force to a kinetochore. kMTs, physically separate from the motor system, would assemble and disassemble, governing the conversion of the contractile forces into chromosome motion. To account for the microbeam results presented here, the amount of contractile machinery attached to a kinetochore must be proportional to the kinetochore surface area, and damage to a kinetochore must reduce the strength of the contractile motor as well as the number of kMTs.

Mitchison and Kirschner (26) and Gorbsky et al. (9) have shown that subunits are lost from kMTs during anaphase primarily at the kinetochores and not at the poles as predicted by traction fiber models (9, 44). Also, when cells in prometaphase are treated with the microtubule inhibitor nocodazole to induce kinetochore fiber shortening, subunits appear to be lost from the kinetochore end of the microtubules (4). These data support the concept that motors for anaphase A, and perhaps prometaphase, are located at or near the kinetochore and that kinetochores may be more actively involved in mitosis than previously recognized (for discussion see references 24, 32, 44).

Recent observations of chromosome behavior on monopolar spindles suggest a new perspective on prometaphase congression, whatever the poleward force-producing mechanism is (41, 43, 44). Chromosomes associated with a monopolar spindle have a single fiber attached to the pole-facing kinetochore. The distal kinetochore, which has no attached microtubules, is inactive (41). All of the chromosomes should

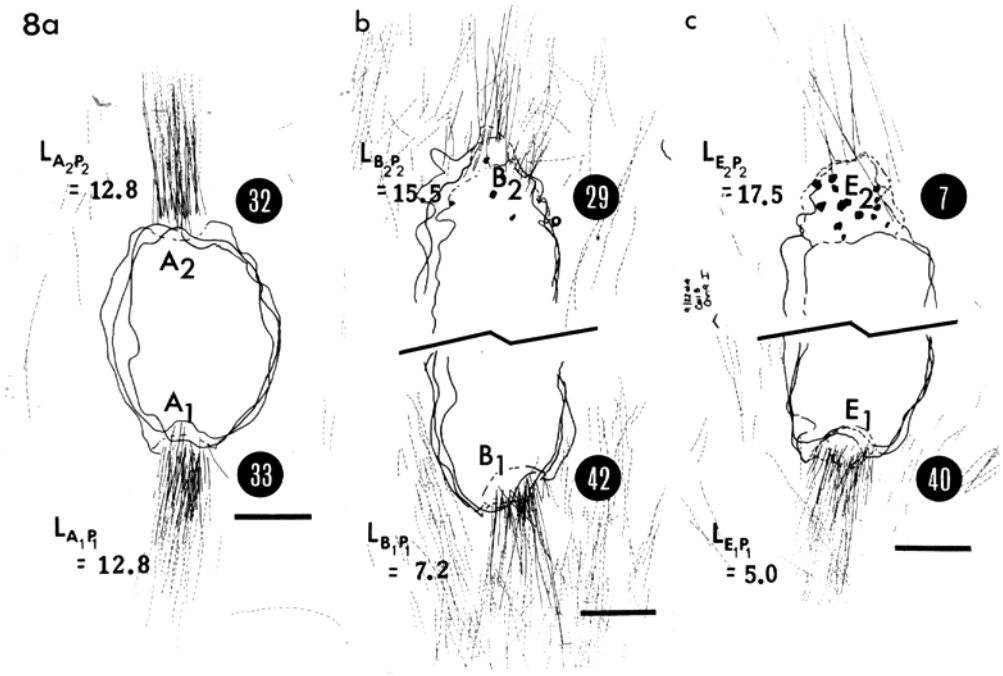

Figure 8. Comparison of microtubule number and kinetochore fiber lengths for irradiated vs. unirradiated chromosomes for three of the bivalents in cell 2 (see Table I and Fig. 6). (*a*) For an unirradiated bivalent, A, kinetochore fiber lengths $L_{A_1P_1}$ and $L_{A_2P_2}$ are equal as are the kMT numbers for kinetochores A_1 and A_2 (numbers in circles). (*b* and *c*) For irradiated bivalents B and E, the kinetochore fibers associated with the irradiated kinetochores (B_2 and E_2) are longer than the fibers of the nonirradiated kinetochores (B_1 and E_1) or ($L_{B_2P_2} > L_{B_1P_1}$; $L_{E_2P_2} > L_{E_1P_1}$), while the number of microtubules associated with the irradiated kinetochore is smaller than for the unirradiated homologous kinetochore ($kMT\#_{B_2} < kMT\#_{B_1}$; $kMT\#_{E_2} < kMT\#_{E_1}$). Bars, 1 μm.

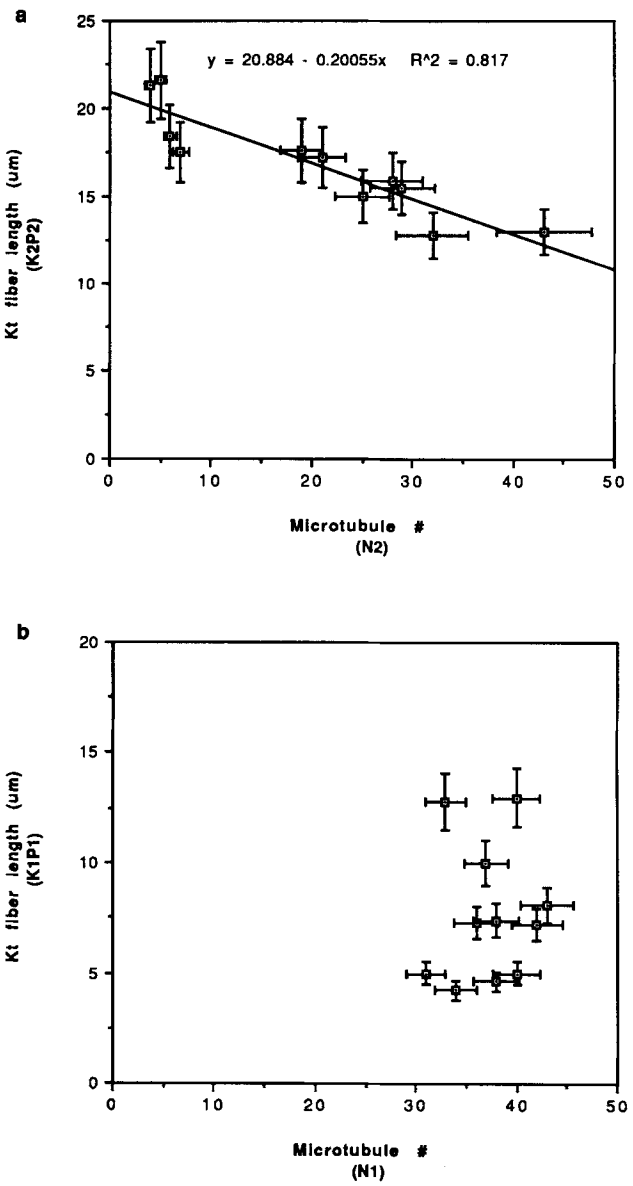

Figure 9. The relationship between kinetochore fiber length and kMT number for irradiated (*a*) and unirradiated (*b*) kinetochores. The values for kinetochore fiber length (kinetochore-to-pole distances, K_1P_1, or K_2P_2) and microtubule number were determined from the reconstruction of serial thin sections. Values are for chromosomes analyzed in cells 1–4; see Table I. The solid line in *a* is from a regression analysis (slope = −0.2; r^2 = 0.82). For irradiated kinetochores, kinetochore fiber length is inversely dependent on the number of microtubules remaining attached to the damaged kinetochore. Kinetochore fiber lengths for unirradiated kinetochores are independent of kMT number.

be pulled into the spindle pole if the only forces acting on the chromosome were poleward forces at the kinetochore, no matter whether the kinetochore force was produced by traction fibers, contractile elements, or kinetochore-associated motors. Instead, chromosomes associated with monopolar spindles frequently lie at a distance from the pole that is typical of bipolar spindles (1, 20, 41, 43). In monopolar spindles, the oscillatory movements of chromosomes and their positions relative to the spindle pole appear to result from their being pushed outward by the array of microtubules emanating from the single pole (41). "Polar-ejection forces" or "elimination forces" as originally described by Ostergren (37) also exist in bipolar spindles, as inferred from the movements of mono-oriented chromosomes and the orientation and ejection of chromosome arms and acentric chromosome fragments (41, 44).

An explanation for the balancing of forces during prometaphase congression can be constructed with a combination of kinetochore motors pulling chromosomes poleward against antagonistic polar ejection forces (5, 41, 43). The congression of chromosomes cannot be explained easily by models where kinetochore motors pull on microtubules and the poleward force on a chromosome depends solely on the number of kMTs (16), because poleward force at the kinetochore then is independent of the distance from the pole. If this were the case, an unbalanced number of kMTs between homologous kinetochore complexes would cause the bivalent to travel all the way to the pole that had the greater number of microtubules. Our data show that this does not occur.

One important assumption is that the strength of the ejection force produced by a polar array of microtubules is maximum near the spindle pole and decreases with distance away from the pole, becoming zero at a distance typical of the interpolar length of metaphase spindles. A poleward motor at the kinetochore in combination with polar ejection forces on the chromosome could provide a model of mitosis in which the basic mechanism of assembly of the polar microtubules in mitosis is essentially the same as that in the interphase cell (5; for a detailed discussion see reference 43). Mechanisms for treadmilling of tubulin subunits or mechano–chemical cross-links along kMTs are not needed. The action is at the

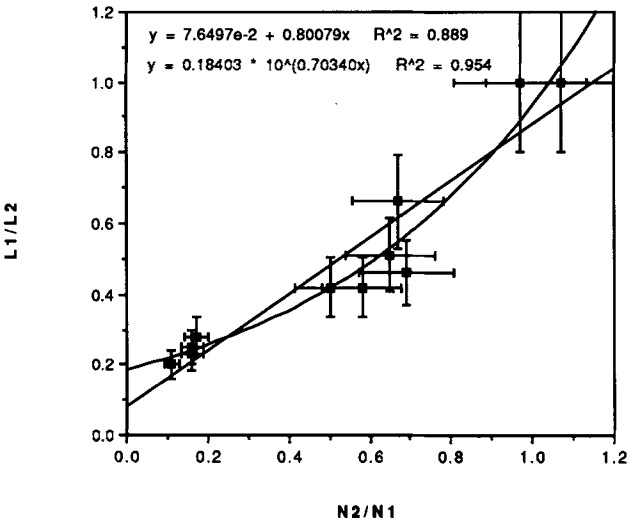

Figure 10. The relationship between microtubule number and kinetochore fiber length for irradiated vs. unirradiated kinetochores. To normalize values, the ratios of the kinetochore fiber lengths (L_1/L_2) are plotted against the ratios of kMT numbers (N_2/N_1). The subscripts 1 and 2 refer to the two opposed, homologous kinetochores. The regression analysis compares the fit of the data to a straight line (r^2 = 0.89), and an exponential curve (r^2 = 0.95). At congression equilibrium, the magnitude of force on a kinetochore is a function of both kMT number and fiber lengths as predicted by $L_1N_1 = L_2N_2$ or $L_1/L_2 = N_2/N_1$.

kinetochore and the chromosome. Poleward force may be generated by dynein-like ATPases associated with the kinetochore (40, 54; for reviews see references 22, 44) or by the energy released from the depolymerization of kMTs at the kinetochore (16). A mechanistic model of chromosome congression based on the above assumptions has been shown to provide a close fit to our data in Fig. 10 (for details see reference 43). However, the magnitude of polar ejection forces has not been measured, and the assumption that these forces decrease with distance from the pole remains to be tested. Also, this model depends on the untested assumption that the forces acting on a chromosome within a bipolar spindle are simply the sum of the forces generated by two monopolar spindles.

Summary

Our results show that the poleward force at a kinetochore depends on the functional size of a kinetochore as measured here by the number of kMTs. The microbeam data is consistent with force-balance models of chromosome congression, but cannot define specifically the molecular mechanisms involved. The results demonstrate, however, that the poleward force at a kinetochore is directly related to the number of kMTs and the kinetochore-to-pole distance.

We acknowledge many useful discussions with Drs. Bruce Nicklas, Donna Kubai, Albert Harris, and Michael Berns during the course of this work. Thanks is extended to Dr. Bruce Nicklas for generously providing time on the aerial viewer for analysis of electron micrographs. We acknowledge Andrea McKibbins for technical assistance in the analysis and reconstruction of serial micrographs. We are grateful to Mike Koonce and Robert Walter for technical assistance in the use of the laser microbeam facility at the University of California at Irvine. The editing of Nancy Salmon is greatly appreciated.

The Laser Microbeam Program is directed by Dr. Michael Berns and supported by National Institutes of Health (NIH) grant RR 01192 as a National Biotechnological Resource. This work was also supported by NIH grant GM24364 to E. D. Salmon.

Received for publication 31 January 1989 and in revised form 6 October 1989.

References

1. Bajer, A. S. 1982. Functional anatomy of monopolar spindles and evidence for oscillatory movement in mitosis. *J. Cell Biol.* 93:33–48.
2. Begg, D. A., and G. W. Ellis. 1979. Micromanipulation studies of chromosome movement. I. Chromosome-spindle attachment and the mechanical properties of chromosome spindle fibers. *J. Cell Biol.* 82:528–541.
3. Berns, M. W., J. Aist, J. Edwards, K. Struhs, J. Girten, P. McNeill, J. B. Rattner, M. Kitzes, M. Hammer-Wilson, L. -H. Liaw, A. Siemens, M. Kounce, S. Peterson, S. Brenner, J. Burt, R. Walter, P. J. Bryant, D. VanDyk, J. Coulombe, T. Cahill, and G. S. Berns. 1981. Laser microsurgery in cell and developmental biology. *Science (Wash. DC).* 213: 505–513.
4. Cassimeris, L. N. 1988. Microtubule assembly dynamics in vivo. Ph.D. thesis. University of North Carolina, Chapel Hill, NC.
5. Cassimeris, L. U., R. A. Walker, N. K. Pryer, and E. D. Salmon. 1987. Dynamic instability of microtubules. *Bioassays.* 7:149–154.
6. Forer, A. 1985. Does actin produce the force that moves a chromosome to the pole during anaphase? *Can. J. Biochem. Cell Biol.* 63:585–598.
7. Forer, A. 1988. Do anaphase chromosomes chew their way to the pole or are they pulled by actin? *J. Cell Sci.* 91:449–453.
8. Gorbsky, G. J., and G. G. Borisy. 1989. Microtubules of the kinetochore fiber turn over in metaphase but not in anaphase. *J. Cell Biol.* 109:653–662.
9. Gorbsky, G. J., P. J. Sammak, and G. G. Borisy. 1987. Chromosomes move poleward in anaphase along stationary microtubules that coordinately disassemble from their kinetochore ends. *J. Cell Biol.* 104:9–18.
10. Hays, T. S., D. Wise, and E. D. Salmon. 1982. Traction force on a kinetochore at metaphase acts as a linear function of kinetochore fiber length. *J. Cell Biol.* 93:374–382.
11. Heath, I. B. 1981. Mechanisms of nuclear division in fungi. *In* The Fungal Nucleus. K. Gull and S. Oliver, editors. Cambridge University Press, New York. 85–112.
12. Hill, T. L., and M. W. Kirschner. 1982. Bioenergetics and kinetics of microtubule and actin filament assembly-disassembly. *Int. Rev. Cytol.* 78:1–125.
13. Hiramoto, Y., Y. Hamaguchi, Y. Shoji, T. E. Schroeder, S. Shimoda, and S. Nakamura. 1981. Quantitative studies on the polarization optical properties of living cells. II. The role of microtubules in birefringence of the spindle of the sea urchin egg. *J. Cell Biol.* 89:121–130.
14. Inoué, S. 1981. Video image processing greatly enhances contrast quality and speed in polarization-based microscopy. *J. Cell Biol.* 83:346–356.
15. Izutsu, K. 1961. Effects of ultraviolet microbeam irradiation upon division in grasshopper spermatocytes. II. Results of irradiation during metaphase and anaphase I. *Mie Med. J.* 11:213–232.
16. Koshland, D. E., T. S. Mitchison, and M. W. Kirschner. 1988. Polewards chromosome movement driven by microtubule depolymerization in vitro. *Nature (Lond.).* 331:499–505.
17. Kubai, D. F. 1973. Unorthodox mitosis in *Trichonympha agilis*: kinetochore differentiation and chromosome movement. *J. Cell Sci.* 13:511–522.
18. Luykx, P. 1970. Cellular mechanisms of chromosome distribution. *Int. Rev. Cytol.* 2(Suppl.):1–173.
19. Margolis, R., and L. Wilson. 1978. Opposite end assembly and disassembly of microtubules at steady state *in vitro*. *Cell.* 13:1–8
20. Mazia, D., N. Paweletz, G. Sluder, and E. M. Finze. 1981. Cooperation of kinetochore and pole in establishment of monopolar mitotic apparatus. *Proc. Natl. Acad. Sci. USA.* 78:377–381.
21. McIntosh, J. R., P. K. Hepler, and D. B. VanWie. 1969. Model for mitosis. *Nature (Lond.).* 244:659–663.
22. McIntosh, J. R., G. P. A. Vigers, and T. S. Hays. 1988. Dynamic behavior of mitotic microtubules. *In* Kinesin, Dynein and Microtubule Dynamics. F. D. Warner and J. R. McIntosh, editors. Alan R. Liss, Inc., New York. 371–382.
23. McNeill, P. A., and M. W. Berns. 1981. Chromosome behavior after laser microirradiation of a single kinetochore in mitotic PtK_2 cells. *J. Cell Biol.* 88:543–553.
24. Mitchison, T. J. 1988. Chromosome alignment at mitotic metaphase: balanced forces or smart kinetochores. *In* Kinesin, Dynein and Microtubule Dynamics. F. D. Warner and J. R. McIntosh, editors. Alan R. Liss Inc., New York. 421–430.
25. Mitchison, T. J. 1989. Poleward microtubule flux in the mitotic spindle: evidence from photoactivation of fluorescence. *J. Cell Biol.* 109:637–652.
26. Mitchison, T. J., and M. W. Kirschner. 1986. Sites of microtubule assembly and disassembly in mitotic cells. *Cell.* 45:515–527.
27. Mizoshima, J., T. Maeda, and T. Miki-Noumura. 1983. Flexural rigidity of singlet microtubules estimated from statistical analysis of their contour lengths and end-to-end distances. *Biochim. Biophys. Acta.* 755:257–262.
28. Nicklas, R. B. 1965. Chromosome velocity during mitosis as a function of chromosome size and position. *J. Cell Biol.* 25:119–135.
29. Nicklas, R. B. 1977. Chromosome movement: facts and hypotheses. *In* Mitosis Facts and Questions. M. P. Little, N. Paweletz, C. Petzelt, H. Ponstingl, D. Schroeter, and H. -P. Zimmerman, editors. Springer-Verlag, New York. 150–155.
30. Nicklas, R. B. 1983. Measurements of the force produced by the mitotic spindle in anaphase. *J. Cell Biol.* 97:542–548.
31. Nicklas, R. B. 1988. The forces that move chromosomes in mitosis. *Annu. Rev. Biophys. Chem.* 17:431–449.
32. Nicklas, R. B. 1988. Chromosomes and kinetochores do more in mitosis than was previously thought. *In* Chromosome Structure and Function: the Impact of New Concepts (18th Stadler Genetics Symposium). J. P. Gustafson and R. Appels, editors. Plenum Press, New York. 53–74.
33. Nicklas, R. B., and G. W. Gordon. 1985. The total length of spindle microtubules depends on the number of chromosomes present. *J. Cell Biol.* 100:1–7.
34. Nicklas, R. B., and C. A. Staehly. 1967. Chromosome manipulation. I. The mechanism of chromosome attachment to the spindle. *Chromosoma (Berl.).* 3:22–47.
35. Nicklas, R. B., B. R. Brinkley, D. A. Pepper, D. F. Kubai, and G. K. Richards. 1979. Electron microscopy of spermatocytes previously studied in life: methods and some observations on micromanipulated chromosomes. *J. Cell Sci.* 35:87–104.
36. Nicklas, R. B., D. F. Kubai, and T. S. Hays. 1982. Spindle microtubules and their mechanical associations after micromanipulation in anaphase. *J. Cell Biol.* 95:91–104.
37. Ostergren, G. 1950. Consideration of some elementary features of mitosis. *Hereditas.* 36:1–19.
38. Pickett-Heaps, J. D. 1986. Mitotic mechanisms: an alternative view. *Trends Biochem. Sci.* 11:504–507.
39. Reider, C. L. 1982. The formation, structure and composition of the mammalian kinetochore and kinetochore fiber. *Int. Rev. Cytol.* 79:1–58.
40. Reider, C. L., and S. P. Alexander. 1989. Kinetochores are transported poleward along a single astral microtubule during chromosome attach-

ment to the spindle in newt lung cells. *J. Cell Biol.* 110:81–95.
41. Reider, C. L., E. A. Davison, L. C. W. Jensen, L. Cassimeris, and E. D. Salmon. 1986. The oscillatory movements of monooriented chromosome, and their position relative to the spindle pole result from the ejection properties of the aster and half-spindle. *J. Cell Biol.* 103:581–593.
42. Salmon, E. D. 1975. Spindle microtubules: thermodynamics of *in vivo* assembly and role of chromosome movement. *Ann. NY Acad. Sci.* 253: 383–406.
43. Salmon, E. D. 1988. A model of metaphase chromosome congression and anaphase poleward movement. *In* Kinesin, Dynein, and Microtubule Dynamics. F. D. Warner and J. R. McIntosh, editors. Alan R. Liss Inc., New York. 431–440.
44. Salmon, E. D. 1989. Microtubule dynamics and chromosome movement. *In* Mitosis, Molecules and Mechanisms. J. S. Hyams and B. R. Brinkley, editors. Academic Press, London. 119–181.
45. Salmon, E. D., and D. A. Begg. 1980. Functional implications of cold-stable microtubules in kinetochore fibers of insect spermatocytes during anaphase. *J. Cell Biol.* 85:853–865.
46. Salmon, E. D., M. McKeel, and T. Hays. 1984. Rapid rate of tubulin dissociation from microtubules in the mitotic spindle *in vivo* measured by blocking polymerization with colchicine. *J. Cell Biol.* 99:1066–1075.
47. Sato, H., G. W. Ellis, and S. Inoué. 1975. Microtubule origin of mitotic spindle form birefringence: demonstration of the applicability of Weiner's equation. *J. Cell Biol.* 67:501–517.
48. Schnapp, C. J., and A. Forer. 1984. Video digitizer analysis of birefringence along the lengths of single chromosomal spindle fibres. *J. Cell Sci.* 65:41–60.
49. Scholey, J. M., M. E. Porter, P. M. Grissom, and J. R. McIntosh. 1985. Identification of kinesin in sea urchin eggs and evidence for its localization in the mitotic spindle. *Nature (Lond.).* 318:483–486.
50. Spurck, T. E., J. D. Pickett-Heaps, and M. W. Klymkowsky. 1986. Metabolic inhibitors and mitosis. I. Effects of dinitrophenol/deoxyglucose and nocodazole on the live spindle. *Protoplasma.* 131:47–59.
51. Tippit, D. H., I. Pillus, and J. D. Pickett-Heaps. 1980. Organization of spindle microtubules in *Ochromonas damica. J. Cell Biol.* 87:531–545.
52. Urtez, R. B., W. Bloom, and R. E. Zirkle. 1954. Irradiation of parts of individual cells. II. Effects of an ultraviolet microbeam on parts of chromosomes. *Science (Wash. DC).* 120:197–199.
53. Vale, R. D., T. S. Reese, and M. P. Sheetz. 1985. Identification of a novel force-generating protein, kinesin, involved in microtubule-based motility. *Cell.* 42:39–50.
54. Vallee, P. B., B. M. Paschal, and H. S. Shpetner. 1989. Characterization of microtubule-associated protein (MAP) 1C as the motor for retrograde organelle transport and its identification as dynein. *In* Kinesis, Dynein and Microtubule Dynamics. F. D. Warner and J. R. McIntosh, editors. Alan R. Liss Inc., New York. 211–222.
55. Wise, D. 1978. On the mechanism of prometaphase congression: chromosome velocity as a function of position on the spindle. *Chromosoma (Berl.).* 69:231–241.
56. Witt, P. L., H. Ris, and G. G. Borisy. 1981. Structure of kinetochore fibers: microtubule continuity and inter-microtubule bridges. *Chromosoma (Berl.).* 83:523–540.